Supplementary Information (SI) for Chemical Communications.

Supplementary Information

Symmetry Breaking Charge Separation in Linked Violanthrone Dimers

Nina I. Novikova, Mina Barzegaramiriolya, Yiheng Lu, Wallace W. H. Wong and Kenneth P. Ghiggino

School of Chemistry and ARC Centre of Excellence in Exciton Science, University of Melbourne, Victoria 3010, Australia

Contents

Materials and Methods

Materials

Unless otherwise indicated, all reagents and solvents were purchased from commercial sources and used without further purification. Violanthrone 79 was purchased from AmBeed Inc., while all violanthrone dimers were synthesised inhouse. Anhydrous dichloromethane (CH_2Cl_2) was obtained from alumina drying columns. Anhydrous dimethylformamide (DMF) were obtained by drying over 4 Å activated molecular sieves. For reactions carried out under inert conditions, standard Schlenk techniques were used. Thin layer chromatography (TLC) was done using Merck-Millipore Silica gel glass plates (60G F254), with a 254 nm and 365 nm light mercury lamp used for identifying spots. Size exclusion chromatography (SEC) was performed using Bio-Beads® S-X1, 200-400 Mesh obtained from Bio-Rad laboratories Inc.

Molecular Structure Characterisation

^{1}H NMR (500 or 600 MHz) and ^{13}C NMR (101, 126, 151 MHz) spectra were acquired with a 500 MHz Agilent DD2 spectrometer, or a 600 MHz Bruker Avance III spectrometer, and chemical shifts were referenced to the residual solvent peaks and is reported as position (δ in ppm), multiplicity (s = singlet, d = doublet, t = triplet, m = multiplet), coupling constant (J in Hz) and integration (number of protons). High-resolution mass spectra were acquired using a Thermo OrbiTrap Exactive Mass Spectrometer.

Steady state spectroscopy

The UV/Vis absorption spectra were acquired using a Cary 50 Bio (Varian) UV-Vis spectrophotometer while PL was measured using fluorescence spectrometer (Cary Eclipse, Agilent Technologies) with excitation at 410 nm and 5 nm excitation and emission bandwidths.

Femtosecond transient absorption

Femtosecond transient absorption spectroscopy experiments were carried out using a custom built pump-probe system with a Yb:KGW femtosecond laser source (Pharos, Light Conversion) producing 50 kHz, 180 fs, 1030 nm pulses. The pump pulses were generated using NOPA (Orpheus-N-2H, Light Conversion) outputting 410 nm, 30 fs pulses, modulated to 25 kHz repetition rate using an optical chopper and set to a magic angle relative to the probe beam using a half wave plate. Probe pulses were generated using an amplifier fundamental beam, focused into a 2 mm sapphire crystal to achieve 500-1000 nm spectral range. The pump beam was focused to a 260 µm spot size and attenuated to achieve 50-75 µJ/cm^2 fluence. Pump and probe beams were overlapped at the sample in a quartz cuvette with a 2 mm path length. The solution was continuously stirred during the experiment to avoid degradation. The transmitted probe was directed into a high repetition rate prism-based spectrometer with a CCD camera (Entwicklungsbuero Stressing, FLC3030). Global analysis of the data was performed using Glotaran software.

Spectroelectrochemistry

A honeycomb spectroelectrochemical (SEC) cell (Pine Research Instruments) was used for SEC measurements with gold mesh as working electrode, gold as counter electrode and silver wire as quasi-reference electrode. A cell was lowered into a quartz cuvette with 2 mm path length containing sample solution. Samples were dissolved in THF with 0.1 M $TBAPF_6$ as electrolyte. A fixed voltage of -1.5 V was applied using a potentiostat (Metrohm Autolab PGSTAT302) and UV/Vis measurements were taken at 15 s intervals using diode-array UV/Vis spectrometer (Agilent 8453).

Fluorescence decay measurements

Fluorescence decay measurements were carried out using the Time correlated single photon counting (TCSPC) technique. An excitation pulse at 410 nm was generated by frequency doubling the 820 nm output from a mode-locked, cavity-dumped Ti/Sapphire laser (Coherent Mira 900F/APE PulseSwitch) pumped by DPSS Nd:YVO_4 laser (Verdi-10, Coherent) and operating at 5.4 MHz. The excitation beam was focused into a 1 cm quartz sample cuvette and fluorescence at magic angle was collected using a hybrid photomultiplier tube (HPM100, Becker & Hickl) after passing through a monochromator (Jobin Yvon H20). Time correlated single photon counting was achieved using a TCSPC module (SPC-150, Becker & Hickl) and decay kinetics were analysed using FAST software (Edinburgh Instruments).

Computational methods and figures

Geometric optimisation were performed using Gaussian 16 software package at a density functional level of theory (DFT). All DFT calculations were carried out using the Becke's three parameter exchange functional with Lee–Yang–Parr correlation functional hybrid method (B3LYP) with Grimme's dispersion correction (D3) and 6-31G(d,p) basis set. Energies of the first 50 singlet and triplet excited states were calculated using TD-DFT on the geometry optimised structure using D3-B3LYP/6-31G(d,p).

Acknowledgment

We would like to acknowledge the support of National Computational Infrastructure (NCI) Australia and the University of Melbourne Spartan High Performance Computing facilities.

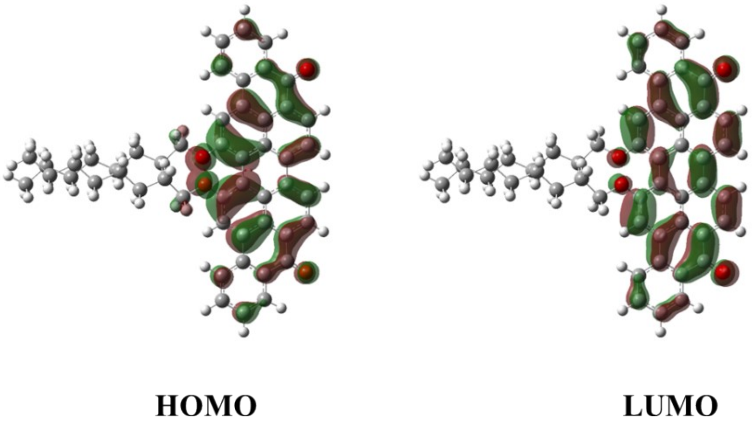

S.I. Fig. 1. The frontier molecular orbitals calculated for V79.

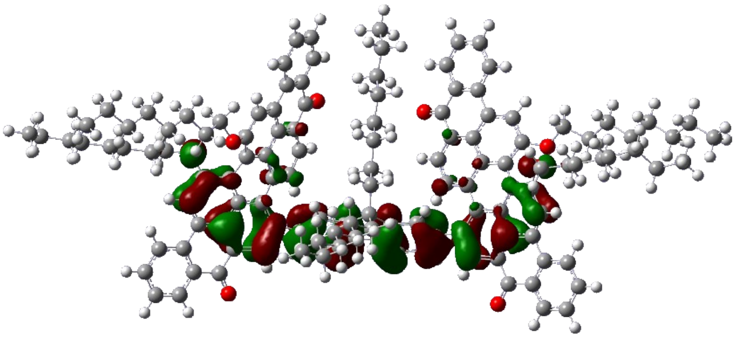

S.I. Fig. 2: The MO calculated for the singlet transition with absorption at 500 nm (HOMO-2 orbital) in dimer I.

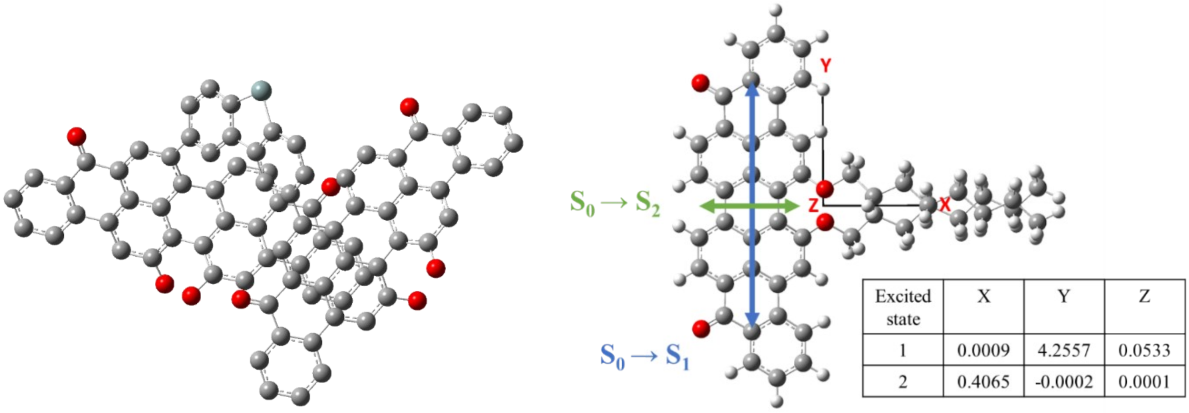

Excited state	X	Y	Z
1	0.0009	4.2557	0.0533
2	0.4065	-0.0002	0.0001

S.I. Fig. 3: Top on view of the DFT optimised structures of dimer II (left) and illustration and vector coordinates of the first two singlet excited state transition dipole moments of V79, calculated using TD-DFT calculations (right).

Synthesis Procedures and Characterisation Data

Synthesis procedures for V79-Cl, V79-Ar and three dimers

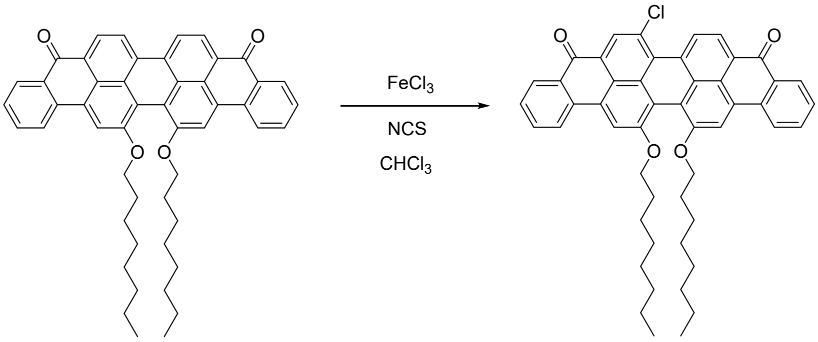

V79-Cl: Violanthrone-79 (V79) (500 mg, 0.7mmol) in $CHCl_3$ (5 ml) was added $FeCl_3$ (113.54 mg, 0.7 mmol) and to this mixture NCS (187 mg, 1.4 mmol) was added portion wise. The reaction stirred overnight refluxed at 60 ˚ C, then cooled to room temperature, added 10ml HCl (1M), extracted with chloroform(2x3mL) and dried over $MgSO_4$. Solvent was evaporated to afford V79-Cl as dark blue solid (501 mg, 95%). RF=0.2 (CH_2Cl_2)

^{1}H NMR (400 MHz, $CDCl_3$) δ 9.14 (d, 1H), 8.58 (s, 1H), 8.48 (d, 2H), 8.43 (dd, 2H), 8.35 (dd, 2H), 8.19 (d, 1H), 7.80 (m, 2H), 7.58 (m, 2H), 4.30 – 4.26 (m, 2H), 4.24 – 4.20 (m, 2H), 1.95 – 1.79 (m, 4H), 1.45 – 1.26 (m, 22H), 0.90 – 0.80 (m, 6H).

^{13}C NMR (151 MHz, $CDCl_3$) δ 182.17, 181.63, 155.82, 155.51, 135.08, 135.04, 133.19, 133.04, 131.22, 131.13, 131.03, 130.68, 130.41, 130.03, 129.50, 129.48, 128.29, 128.23, 127.98, 127.92, 127.12, 126.99, 126.93, 126.87, 126.22, 124.76, 122.85, 122.71, 121.95, 120.58, 115.88, 115.54, 111.95, 111.12, 77.28, 77.07, 76.86, 69.35, 68.98, 31.86, 31.75, 29.74, 29.69, 29.50, 29.42, 29.27, 26.03, 25.93, 22.72, 22.62, 14.15, 14.06.

HRMS (ESI): m/z = 747.3218 ($[M+H]^+$ requires 747.3241 for $C_{50}H_{48}ClO_4$)

Structure assignment for V79-Cl

Comparing the ^{1}H NMR spectrum of V79-Cl with that of violanthrone, we noticed several changes (see S.I. Fig. 4 and S.I. Fig. 5).

1. The relative integration for most downfield doublet signal at 8.61ppm, which was assigned to proton 'g' in V79, was halved. This can be the result of substitution at the 'f' position.
2. A singlet at 8.12ppm emerged and 3 doublet signals around it all had similar relative integration. This again is consistent with the substitution of a proton at position 'f' which decreased the symmetry of the molecule.
3. Doublet 'd', triplet 'b' and triplet 'a' all showed split signals, but remain at similar chemical shifts. Considering V79 is a symmetrical molecule with a C2 axis, the split signals can be a result of chlorination breaking the symmetry. The mass spectroscopy data indicate a mono-chlorination has taken place with m/z = 747.32 ($[M+H]^+$ requires

747.32 for $C_{50}H_{48}ClO_4$). Since the peak type of proton ‘a’, ‘b’, ‘c’, and ‘d’ did not change. We proposed that chlorination should have taken place at proton ‘e’, ‘f’ or ‘g’.

Based on the first and second findings we were able to identify that chlorination happened at position ‘f’. Our argument is the following. If chlorination took place at position ‘e’, the peak type of proton ‘a’ would change from a triplet to a doublet. Therefore, substitution at position ‘e’ can be ruled out. Position ‘f’ and ‘g’ were both possible positions considering the peak types and chemical shift. However, based on our chlorination experiments we would argue that chlorination took place at position ‘f’. When optimizing our chlorination conditions, we found that adding excess equivalence of NCS (up to 20 equivalence) did not result in multiple chlorination. An explanation of this observation is that chlorination at position ‘f’ caused significant steric hinderance preventing further chlorination. In addition, computational data suggested that ‘f’ position has the strongest HOMO character, making it the most facile position for electrophile substitutions (S.I. Fig. 1). Finally, we note that 2D NMR experiments did not provide further insights into the structure assignment.

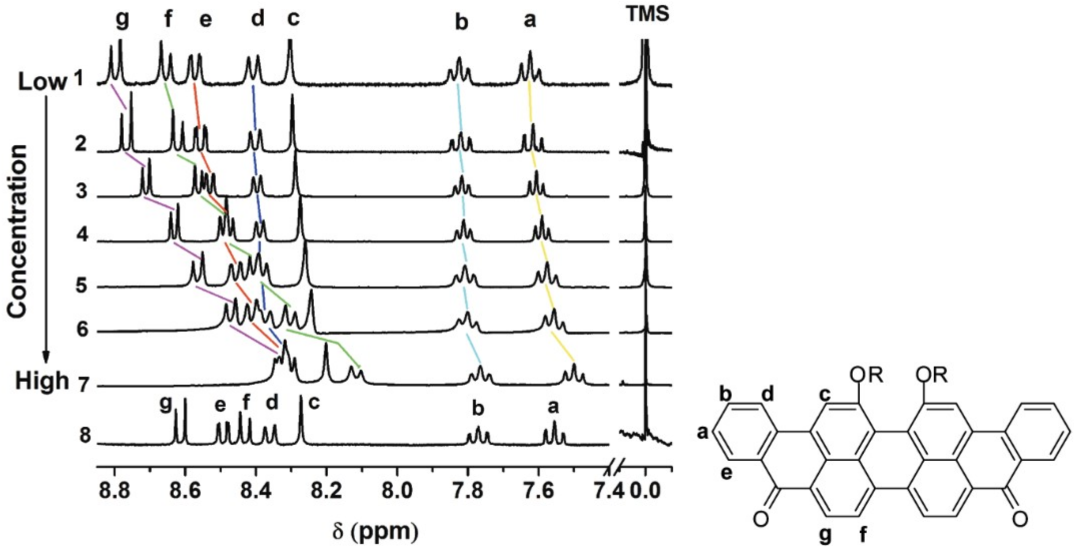

S.I. Fig. 4. ^{1}H NMR spectrum of V79 under different concentrations. Picture is adapted from *J. Phys. Chem. B* **2010**, (115), 618-623. We verified our V79 sample has the same ^{1}H NMR spectrum.

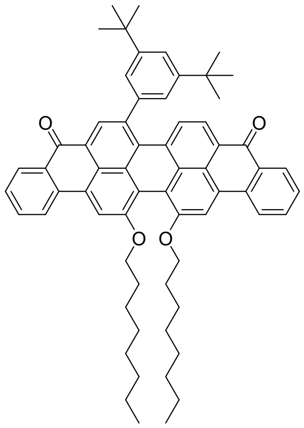

V79-Ar: A microwave vial was charged with a magnetic stir bar, V79-Cl (200 mg, 0.267 mmol), (3,5-Di-tert-butylphenyl) Bpin (169 mg, 0.535 mmol), Cy3P.HBF$_4$ (59.1 mg, 0.16 mmol), Pd$_2$(dba)$_3$ (61.3 mg, 0.067 mmol, 6 mol%). The vial was evacuated and refilled with nitrogen (three times). Under a nitrogen flow, degassed K$_3$PO$_4$ (1 ml, 2M aq solution) were added, followed by degassed THF (5 mL) by syringe. The viol was then heated at 100 ºC and the reaction mixture was stirred for 24 h. The reaction mixture was then cooled to room temperature, the extra amount of THF was evaporated and the crude passed through a short silica plug and washed with toluene, concentrated in vacuo and purified via layered recrystallization using mixture of CH$_2$Cl$_2$ and isopropanol to afford the final compound as a blue solid (170 mg, 75%).

^{1}HNMR (600 MHz, CDCl$_3$) δ 8.79 (s, 1H), 8.57 (d, *J* = 7.7 Hz, 1H), 8.52 (d, *J* = 7.7 Hz, 1H), 8.45 – 8.37 (m, *J* = 18.3, 9.2 Hz, 2H), 8.32 (s, 1H), 8.28 (s, 1H), 8.19 (d, *J* = 8.1 Hz, 1H), 7.84 – 7.76 (m, *J* = 17.8, 8.9 Hz, 2H), 7.71 (d, *J* = 8.1 Hz, 1H), 7.64 – 7.56 (m, *J* = 14.9, 7.4 Hz, 2H), 7.46 (s, 1H), 6.88 (s, 1H), 4.39 – 4.16 (m, 4H), 1.99 – 1.78 (m, 4H), 1.65 – 1.16 (m, 32H), 1.15 – 0.93 (m, 8H), 0.91 – 0.76 (m, 6H).

^{13}C NMR (151 MHz, CDCl$_3$) δ 183.46, 183.09, 156.33, 156.24, 142.23, 142.02, 135.76, 135.70, 134.51, 133.23, 133.04, 132.93, 131.22, 131.08, 131.05, 131.03, 130.80, 129.63, 128.50, 128.39, 128.30, 128.23, 127.28, 127.24, 127.18, 126.66, 125.45, 123.14, 123.11, 122.35, 121.62, 117.60, 116.80, 112.98, 112.41, 69.72, 31.80, 31.77, 31.69, 31.42, 31.19, 29.93, 29.77, 29.52, 29.47, 29.29, 26.12, 26.05, 22.66, 22.64, 14.09, 14.06.

HRMS (ESI): m/z = 901.5100 ([M+H]$^+$ requires 901.5117 for C$_{64}$H$_{68}$O$_4$)

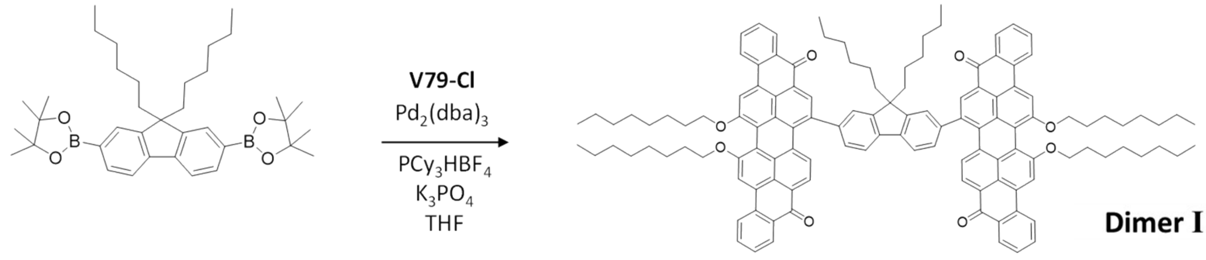

Dimer I

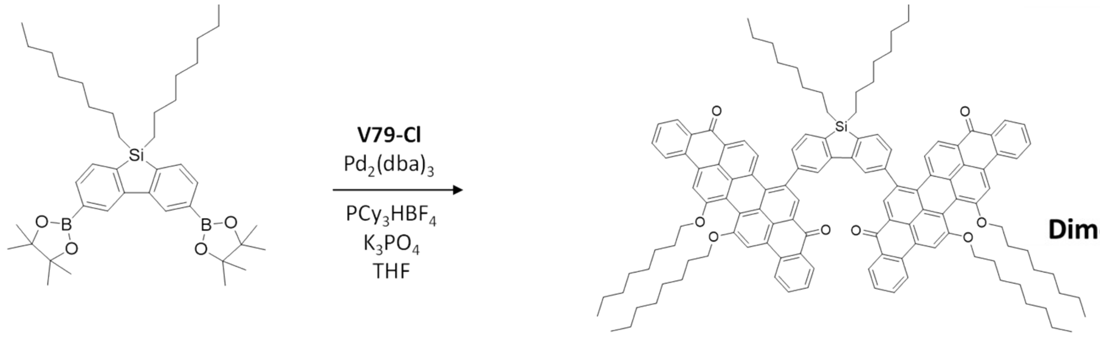

Dimer II

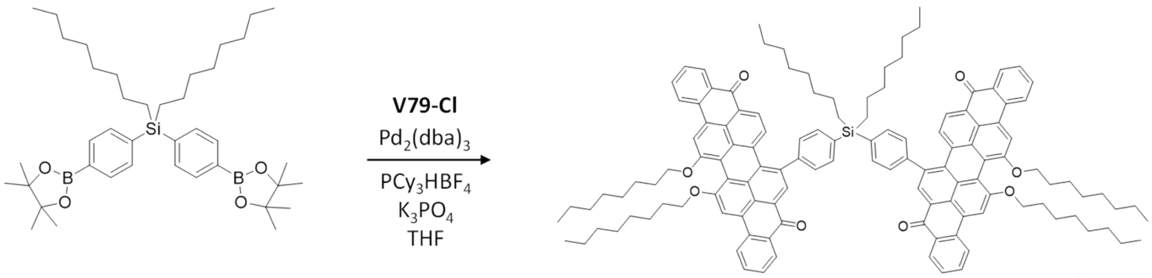

Dimer III

Dimer I: A microwave vial was charged with a magnetic stir bar, V79-Cl (20 mg, 26.7 µmol), 9,9-Dihexyl-9H-fluorene-2,7-diboronic acid bis(pinacol) ester (7.8 mg, 13.4 µmol), $Cy_3P.HBF_4$ (2.37 mg, 6.42 µmol), $Pd_2(dba)_3$ (4.9 mg, 5.35 µmol, 6 mol%). The vial was evacuated and refilled with nitrogen (three times). Under a nitrogen flow, degassed K_3PO_4 (0.2 ml, 2M aq solution) were added, followed by degassed THF (2 mL) by syringe. The vial was then heated at 100 ºC and the reaction mixture was stirred for 24 h. The reaction mixture was then cooled to room temperature, the extra amount of THF was evaporated and the crude passed through a short silica plug and washed with toluene, concentrated in vacuo and purified via layered recrystallization using mixture of CH_2Cl_2 and methanol. The mixture was further purified using size separation column to afford the final compound as a blue solid (75%).

^{1}H NMR (600 MHz, $CDCl_3$) δ 8.83 (d, *J* = 25.7 Hz, 2H), 8.71 – 8.27 (m, 12H), 8.23 – 8.10 (m, 2H), 8.07 – 7.94 (m,2H), 7.93 – 7.73 (m, 5H), 7.69 – 7.51 (m, 5H), 7.21 – 6.90 (m, 2H), 4.53 – 4.15 (m, 8H), 2.03 – 1.82 (m, 8H), 1.65 – 1.18 (m, 54H), 1.16 – 0.98 (m, 6H), 0.95 – 0.78 (m, 18H).

^{13}C NMR (151 MHz, $CDCl_3$) δ 183.53, 156.54, 156.12, 142.54, 141.31, 140.39, 135.77, 133.25, 131.07, 130.95, 128.52, 128.36, 127.22, 123.32, 123.15, 122.39, 117.72, 116.59, 112.98, 112.46, 69.77, 31.81, 31.77, 29.93, 29.76, 29.71, 29.51, 29.47, 29.29, 26.12, 26.05, 22.67, 22.64, 14.09, 14.06.

HRMS (ESI): m/z =1755.9495 ($[M+H]^+$ requires 1755.9453 for $C_{125}H_{127}O_8$)

Dimer II: A microwave vial was charged with a magnetic stir bar, V79-Cl (100 mg, 133.8 µmol), 9,9-Dioctylsilan-9H-fluorene-3,6-diboronic acid bis(pinacol) ester (44.1 mg, 66.9 µmol), $Cy_3P.HBF_4$ (29.56 mg, 80.28 µmol), $Pd_2(dba)_3$ (61.26 mg, 66.9 µmol). The vial was evacuated and refilled with nitrogen (three times). Under a nitrogen flow, degassed K_3PO_4 (1 ml, 2M aq solution) were added, followed by degassed THF (5 mL) by syringe. The vial was then heated at 100 ºC and the reaction mixture was stirred for 24 h. The reaction mixture was then cooled to room temperature, the extra amount of THF was evaporated and the crude passed through a short silica plug and washed with toluene, concentrated in vacuo and purified via layered recrystallization using mixture of CH_2Cl_2 and methanol. The mixture was further purified using size separation column to afford the final compound as a blue solid (15%).

^{1}H NMR (600 MHz, $CDCl_3$) δ 8.90 (s, 1H), 8.70 (s, 1H), 8.57 (s, 2H), 8.41 (s, 3H), 8.33 (s, 1H), 8.23 (s, 2H), 7.80 (m, 3H), 7.63 (s, 2H), 7.49-6.60 (m, 17H), 4.30 (m, 8H), 2.20-1.91 (m, 8H), 1.60-1.05 (m, 72H), 1.05-0.65 (m, 18H).

^{13}C NMR was not possible to obtain due to solubility.

HRMS (ESI): m/z = 1827.9874 ($[M+H]^+$ requires 1827.9848 for $C_{128}H_{134}O_8Si$)

Dimer III: A microwave vial was charged with a magnetic stir bar, V79-Cl (100 mg, 133.8 µmol), 4,4′-(phenyboronic acid pinacol ester) dioctyl silane (44.2 mg, 66.9 µmol), $Cy_3P.HBF_4$ (29.56 mg, 80.28 µmol), $Pd_2(dba)_3$ (61.26 mg, 66.9 µmol). The vial was evacuated and refilled with nitrogen (three times). Under a nitrogen flow, degassed K_3PO_4 (1 ml, 2M aq solution) were added, followed by degassed THF (5 mL) by syringe. The vial was then heated at 100 ºC and the reaction mixture was stirred for 24 h. The reaction mixture was then cooled to room temperature, the extra amount of THF was evaporated and the crude passed through a short silica plug and washed with toluene, concentrated in vacuo and purified via layered recrystallization using mixture of CH_2Cl_2 and methanol. The mixture was further purified using size separation column to afford the final compound as a blue solid (29%).

^{1}H NMR (600 MHz, $CDCl_3$) δ 8.80 (m, 2H), 8.58 (m, 2H), 8.42 (m, 4H), 8.35 – 8.09 (m, 8H), 7.94 (m, 4H), 7.86 – 7.71 (m, 5H), 7.70 – 7.50 (m, 5H), 7.40 (m, 2H), 4.27 (m, 8H), 1.99 – 1.78 (m, 8H), 1.68 – 1.10 (m, 72H), 0.86 (m, 18H).

^{13}C NMR (120MHz, $CDCl_3$) δ 206.93, 183.29, 156.35, 156.09, 143.26, 140.74, 135.71, 134.05, 133,18, 131.00, 130.07, 128.83, 128.26, 127.12, 123.12, 123.02, 122.42, 117.64, 116.64, 77.26, 73.59, 31.94, 31.78, 31.75, 30.91, 29.49, 29.28, 26.07, 22.72, 22.64, 22.61, 14.14, 14.06, 14.03**.**

HRMS (ESI): m/z = 1830.0033 ($[M+H]^+$ requires 1830.0004 for $C_{128}H_{137}O_8Si$)

NMR spectra

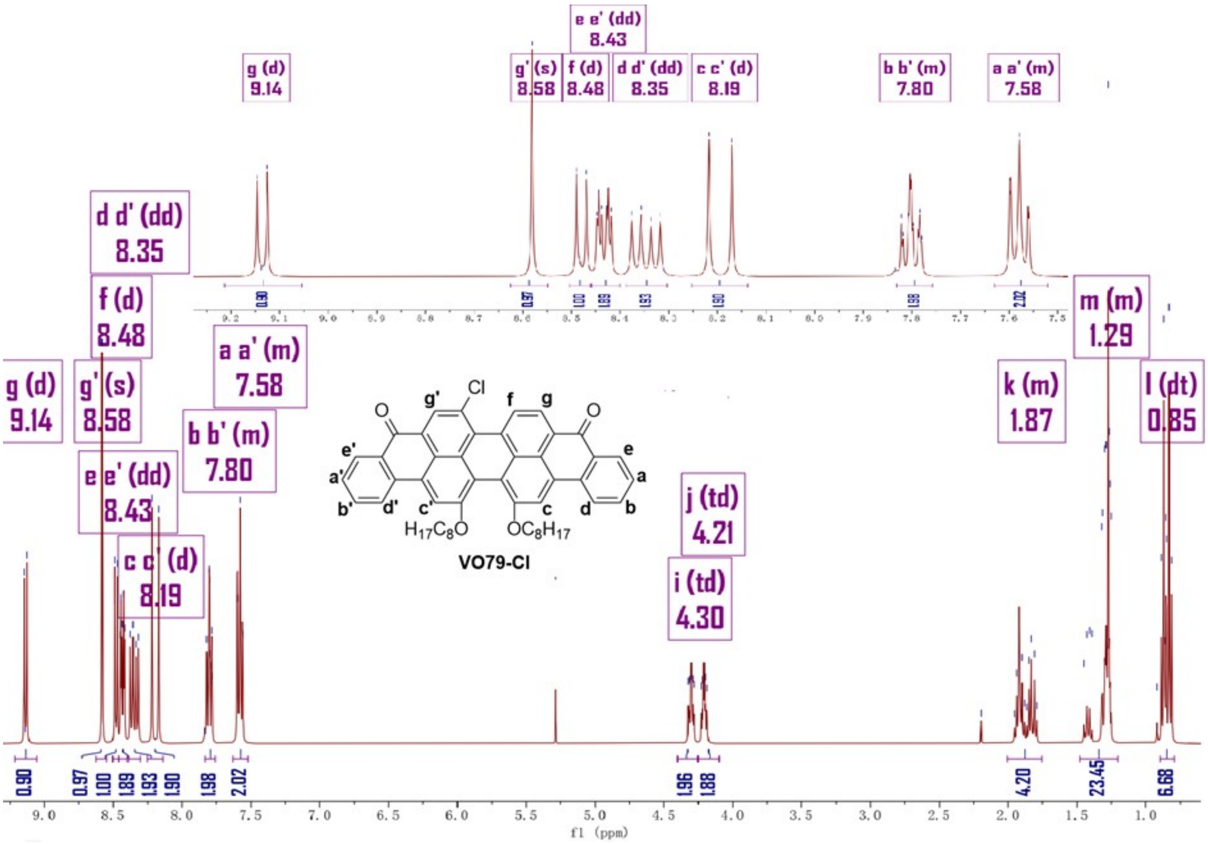

S.I. Fig. 5: ^{1}H NMR spectrum of V79-Cl in $CDCl_3$.

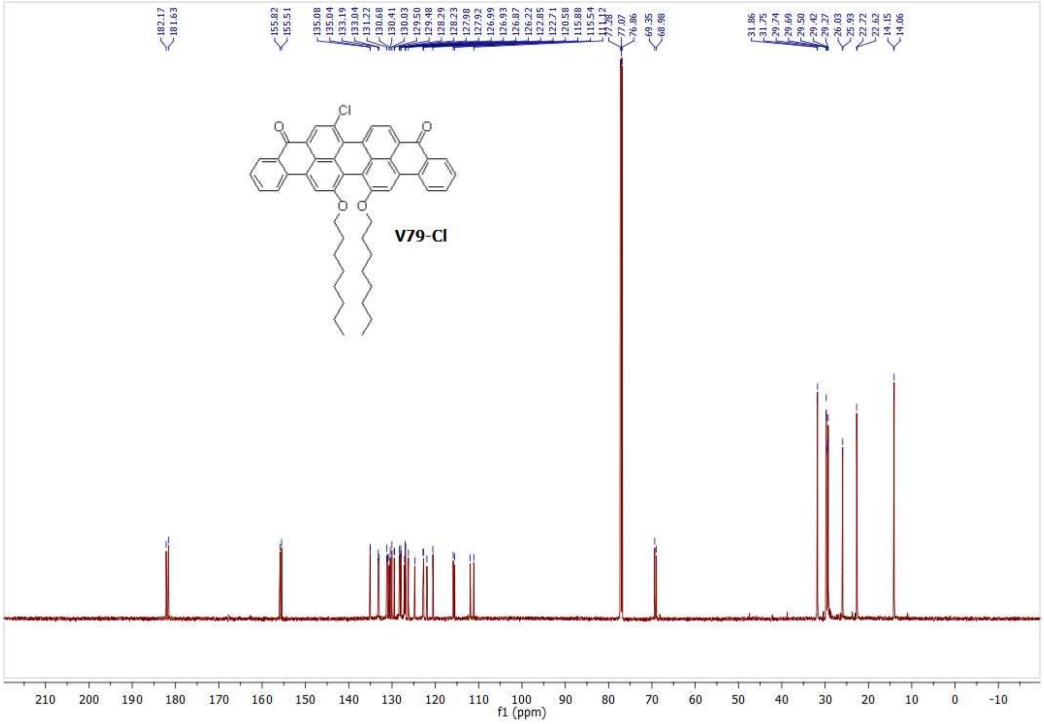

S.I. Fig. 6: ^{13}C NMR spectrum of V79-Cl in $CDCl_3$.

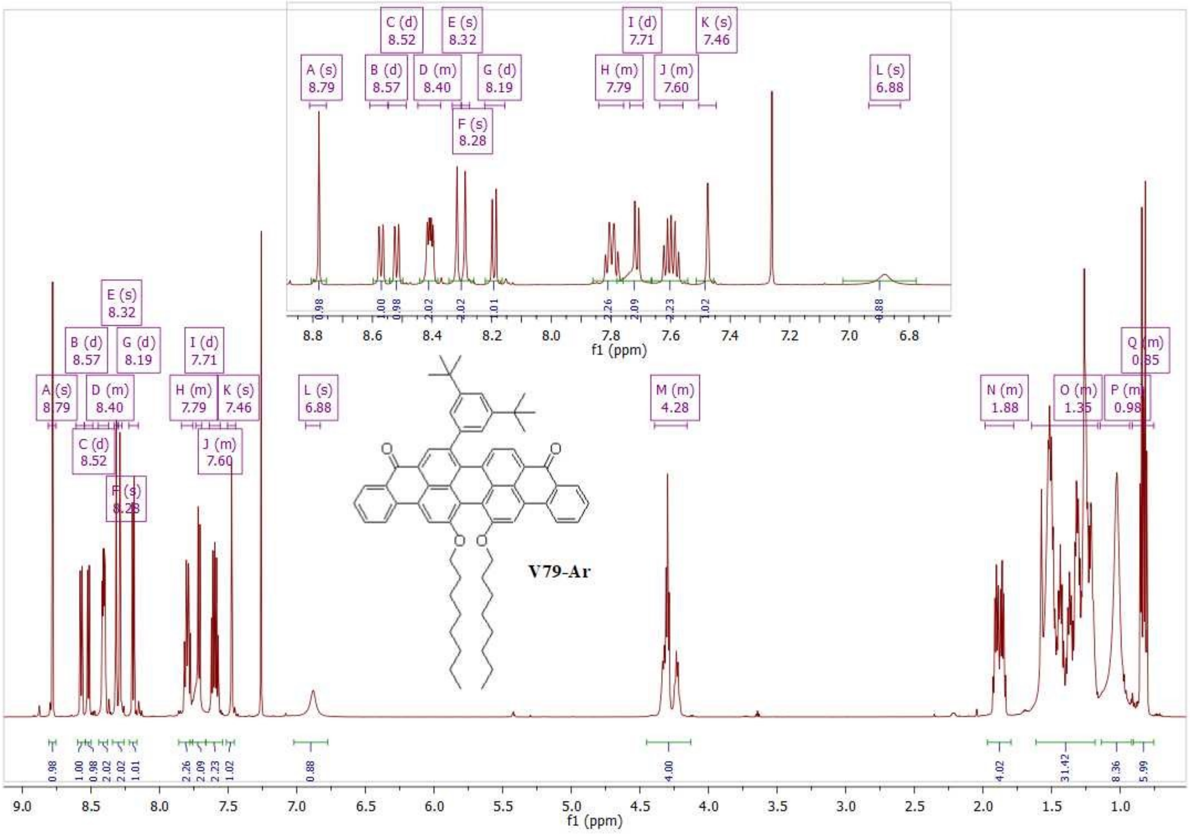

S.I. Fig. 7: ^{1}H NMR spectrum of V79-Cl in $CDCl_3$.

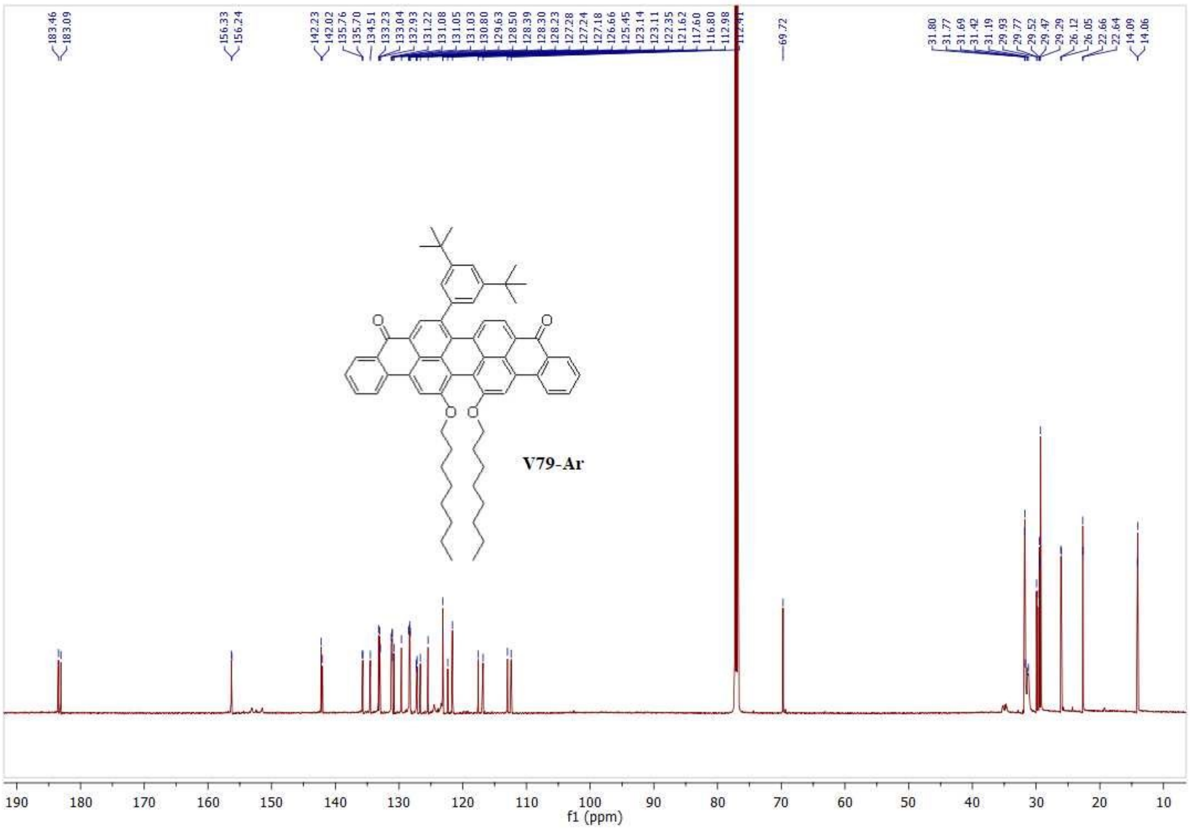

S.I. Fig. 8: ^{13}C NMR spectrum of V79-Cl in $CDCl_3$.

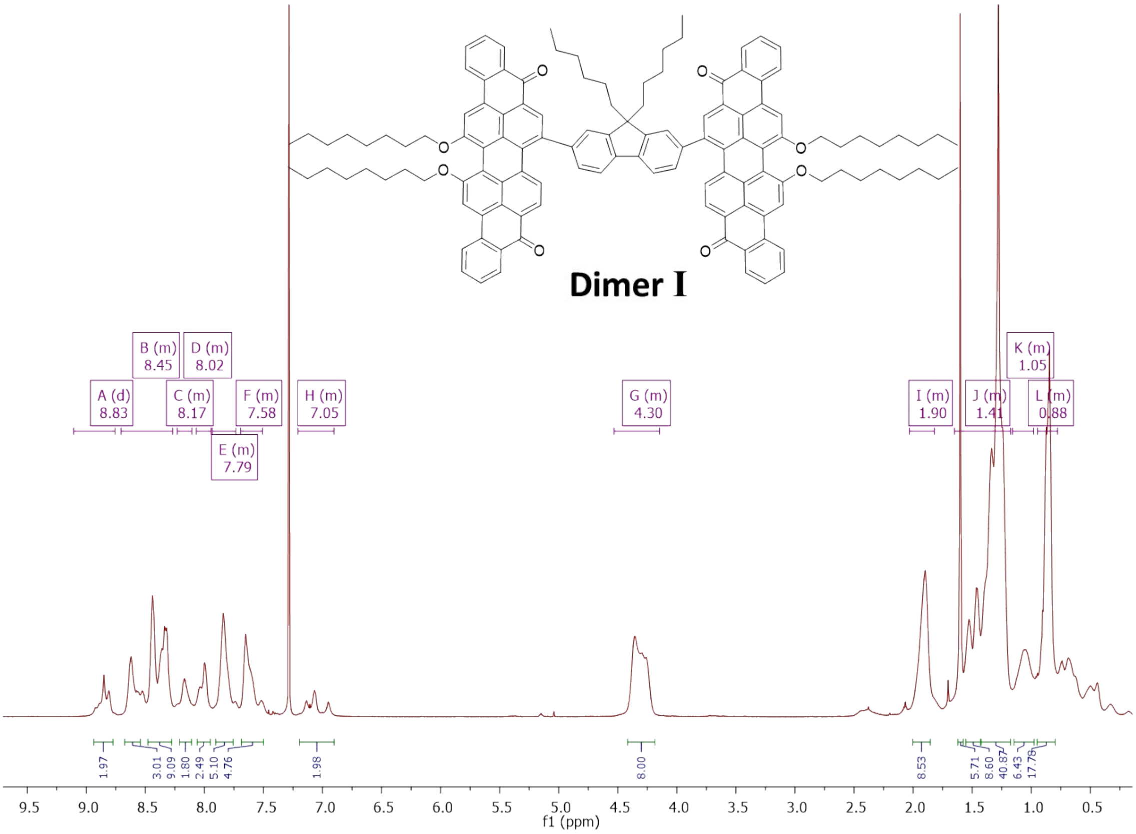

S.I. Fig. 9: ^{1}H NMR spectrum of Dimer I in $CDCl_3$.

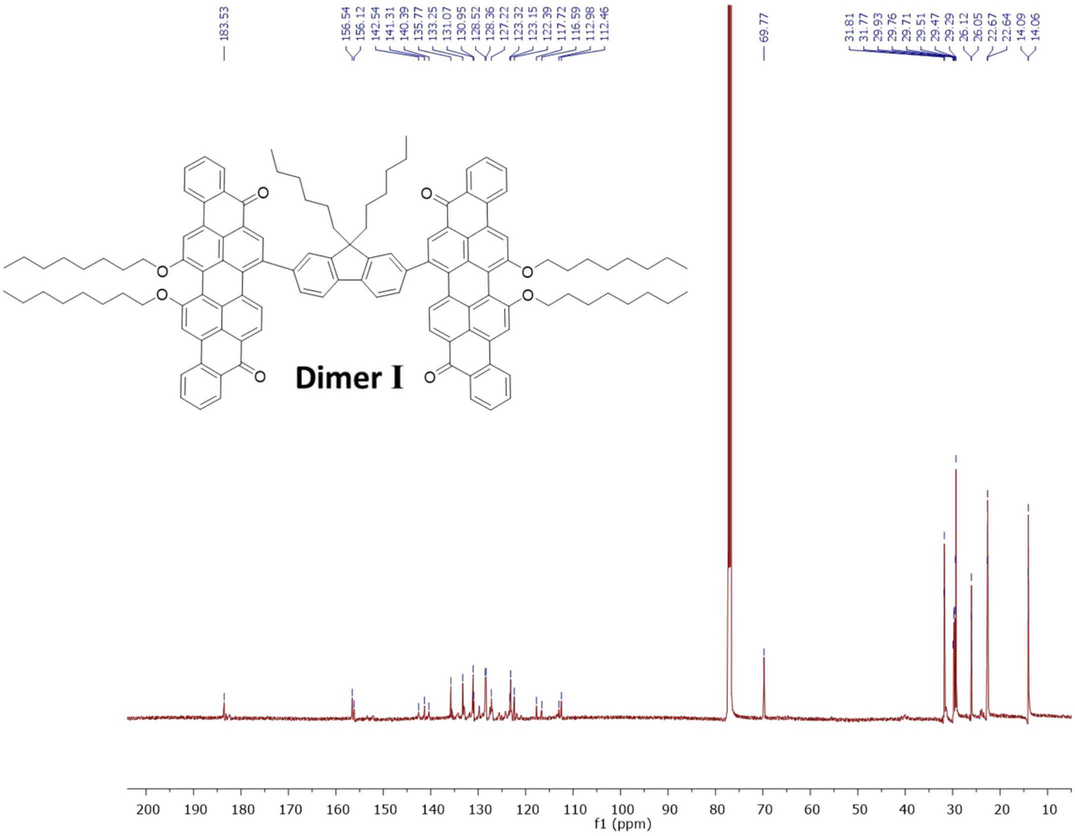

S.I. Fig. 10: ^{13}C NMR spectrum of Dimer I in $CDCl_3$.

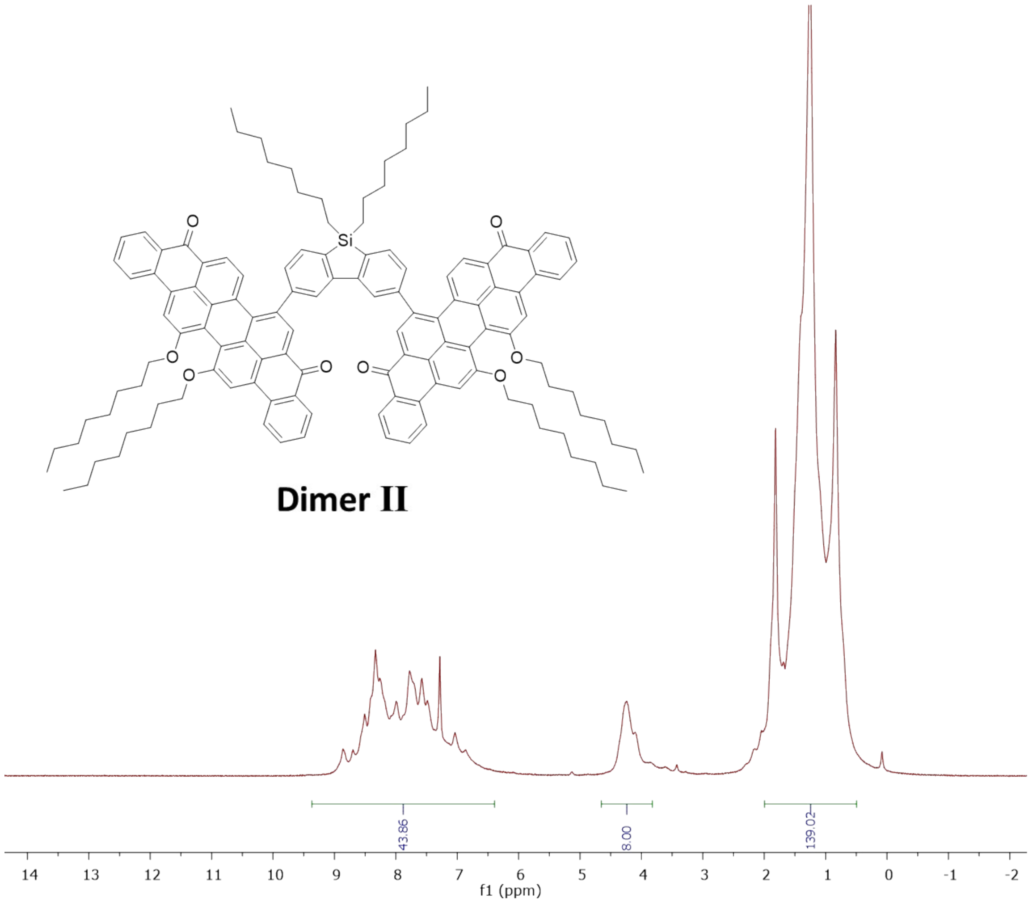

S.I. Fig. 11: ^{1}H NMR spectrum of Dimer II in $CDCl_3$.

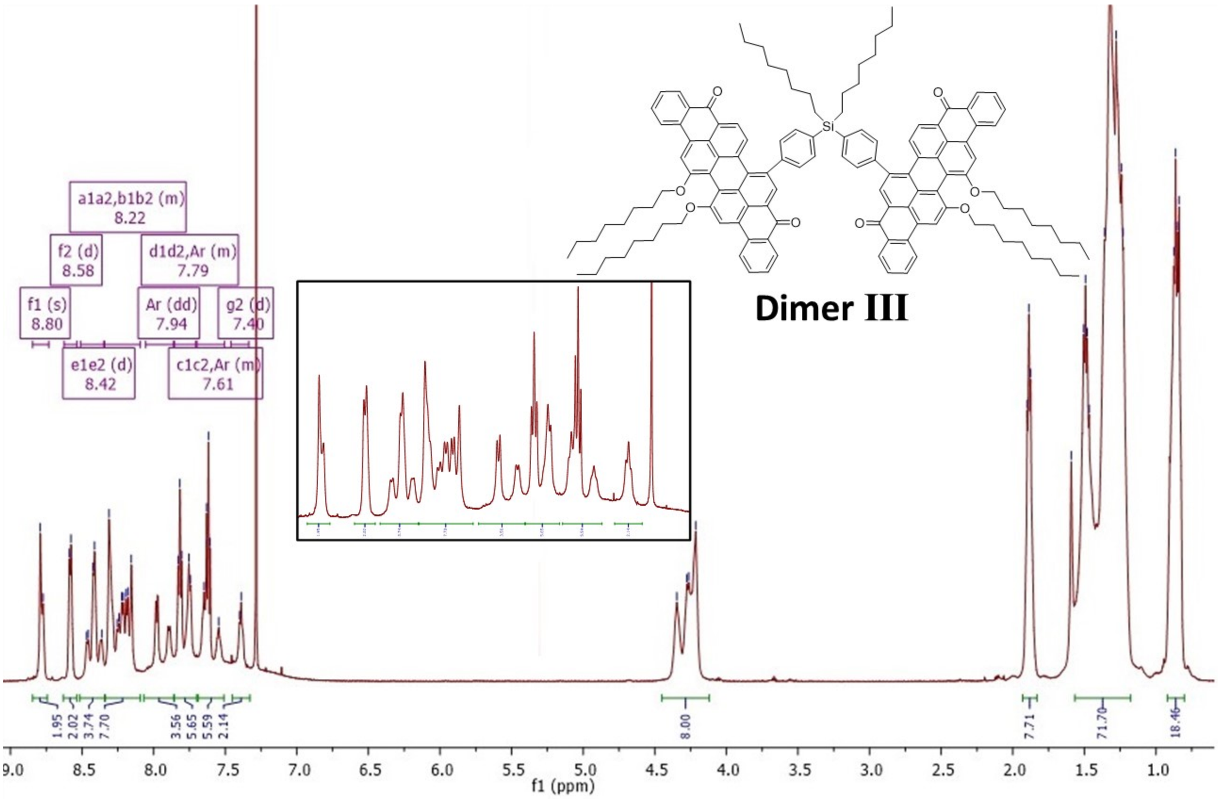

S.I. Fig. 12: ^{1}H NMR spectrum of Dimer III in $CDCl_3$.

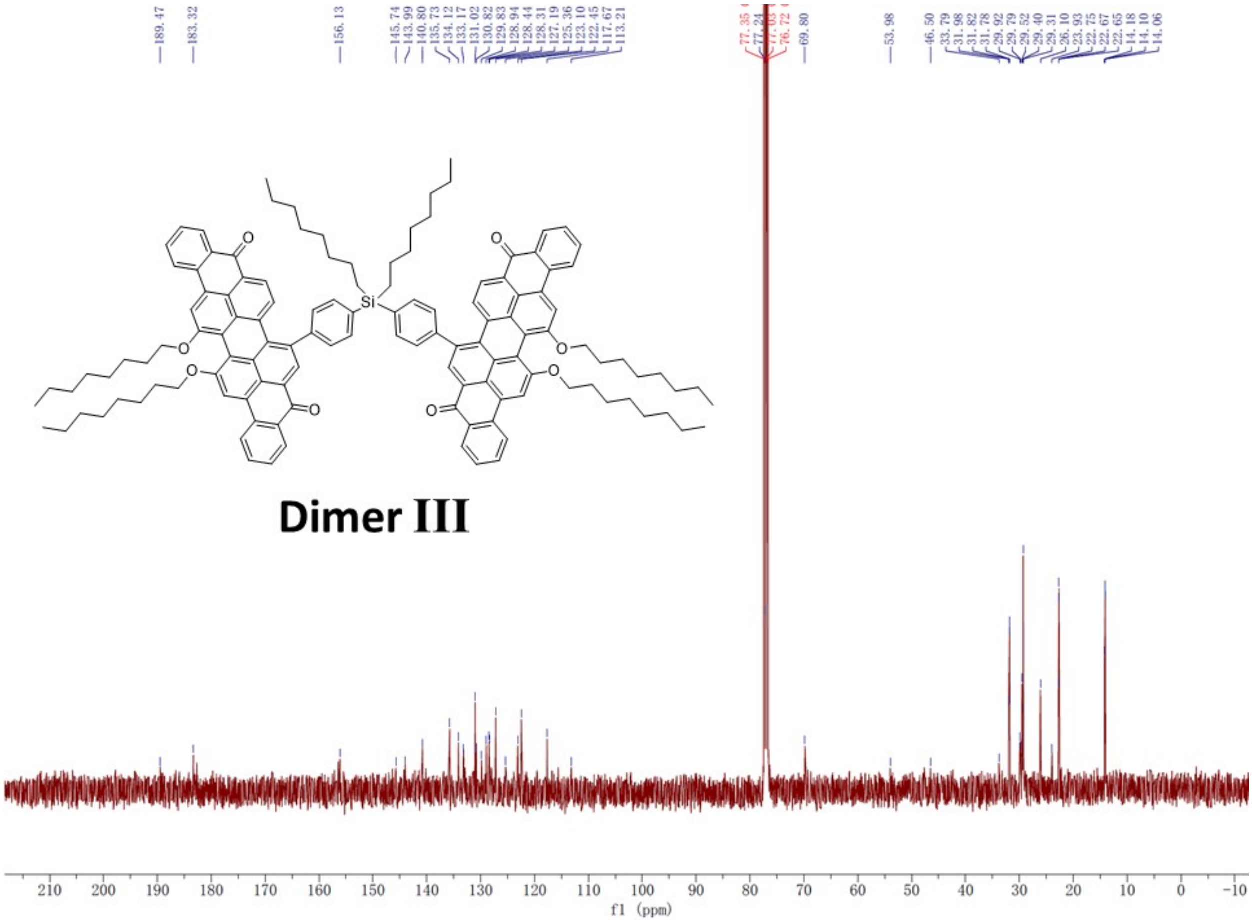

S.I. Fig. 13: ^{13}C NMR spectrum of Dimer III in $CDCl_3$.

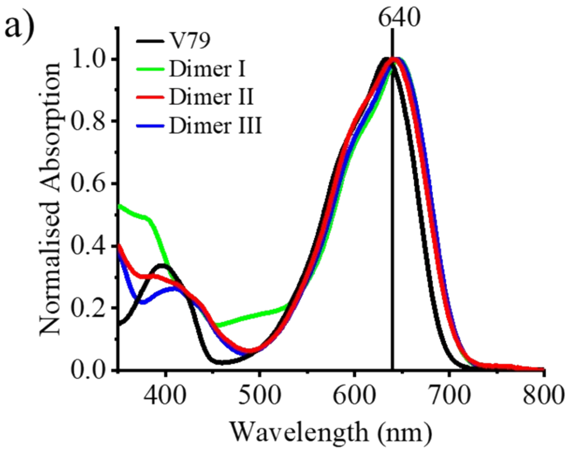

Photophysical Data

S.I. Fig. 14: Normalised UV/Vis absorption of violanthrone monomer and dimers in toluene (a) and benzonitrile (b). Black – violanthrone-79, green -dimer I, red – dimer II, and blue – dimer III. A new absorption band is observed in dimer I at ~500 nm. DFT and TDDFT calculations, assign this band to a transition from HOMO-2 to LUMO, where electron density is delocalized across the aromatic bridge. (S.I. Fig. 2).

S.I. Fig. 15: Normalised experimental and calculated UV/Vis absorption of violanthrone monomer and dimers in toluene and benzonitrile (a) V79 (b) Dimer II (c) calculated UV/Vis spectra of V79 monomer and the three dimers in vacuum.

S. I. Table 1 Photophysical properties of violanthrone compounds in two solvents. Percentage contributions to the lifetime component are indicated in brackets and dominant component

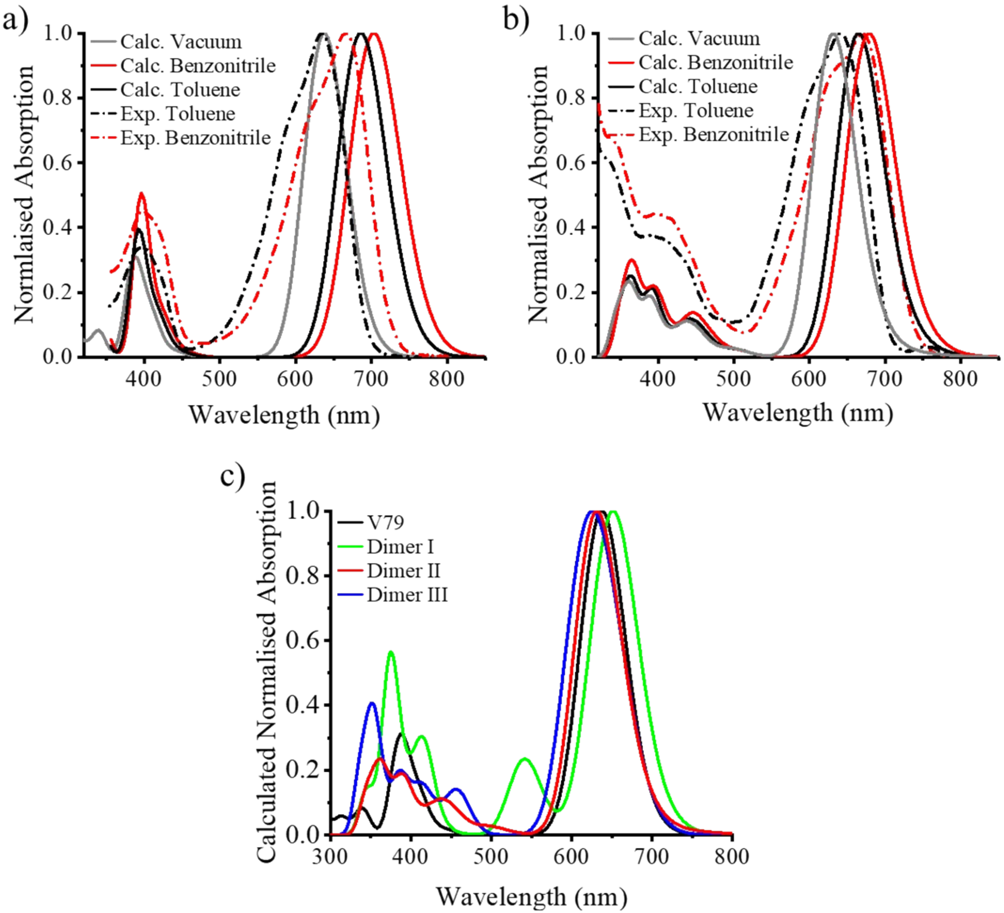

in the signal is indicated in bold. Average radiative rates were calculated using $\langle k_r \rangle = \Phi/\tau_{av}$ where $\tau_{av} = \sum_{i}^{n} B_i \tau_i \Big/ \sum_{i}^{n} B_i$ and B is an amplitude of the component in a multi-exponential decay fit.

		Absorption λ_{max} (nm)	**Emission λ_{max} (nm)**	Φ_{fl}	**τ (ns)**	**k_r (10^7 s^{-1})**
V79	Tol	634	693	0.25	5.46	4.6
	BzCN	666	729	0.06	3.28	1.8
V79-Ar	Tol	644	702	0.26	5.70	4.6
	BzCN	679	738	0.04	3.8	1.1
Dimer I	Tol	646	709	0.21	6.04	3.5
	BzCN	678	740	<0.01	**0.33 (84)**, 0.92 (11), 3.26 (5)	1.8
Dimer II	Tol	640	707	0.18	5.95	3.0
	BzCN	671	743	<0.01	0.21 (22), **0.99 (61),** 2.05 (17)	0.9
Dimer III	Tol	646	707	0.19	4.36 (51), 6.18 (49)	3.6
	BzCN	679	742	0.02	0.91 (36), **2.22 (64)**	1.2

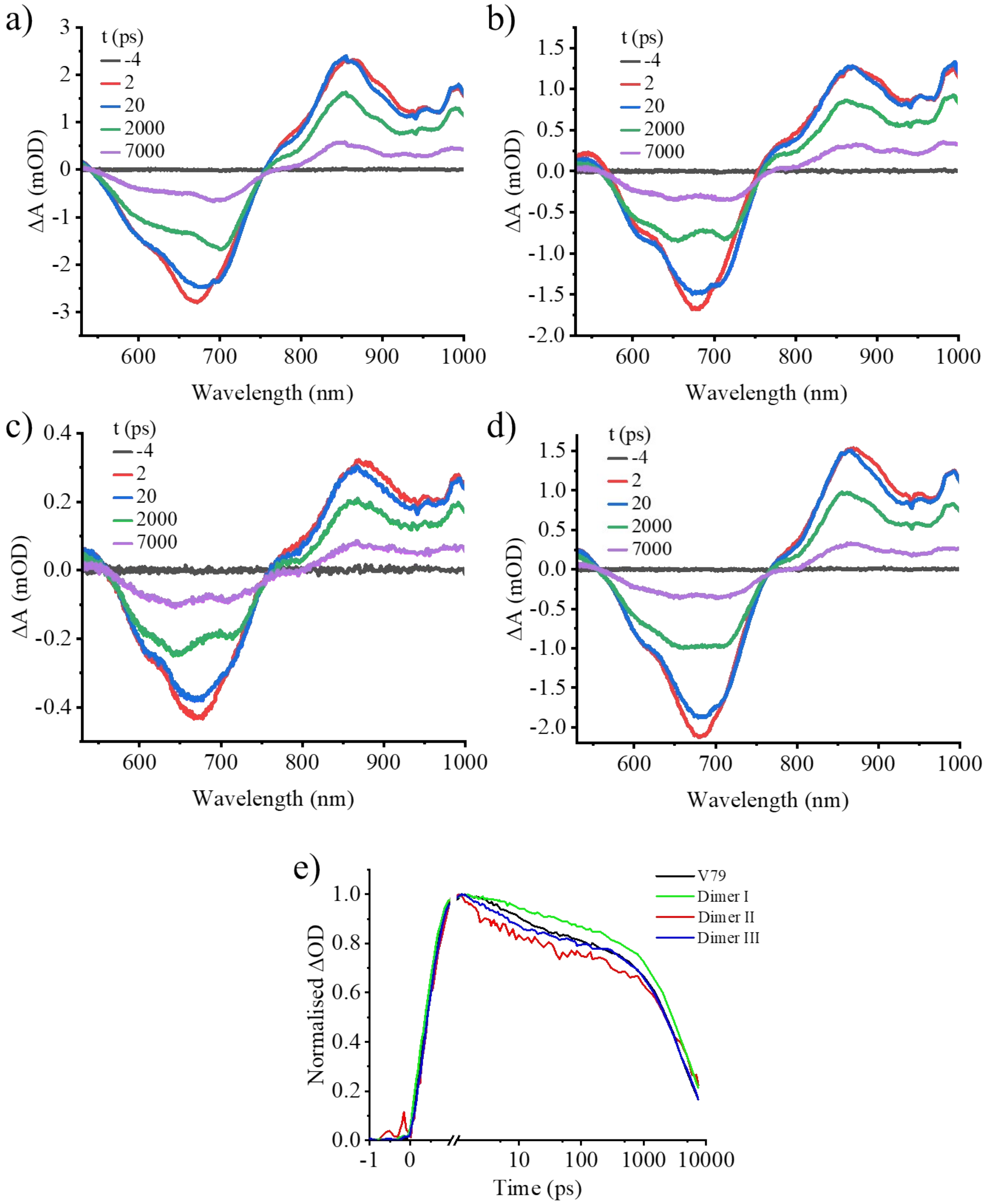

S.I. Fig. 16: Femtosecond transient absorption spectra at select time delays of violanthrone 79 (a), dimer I (b), dimer II (c), dimer III (d), and the kinetic traces of all 4 compounds at 910 nm (e) in toluene with 410 nm excitation.

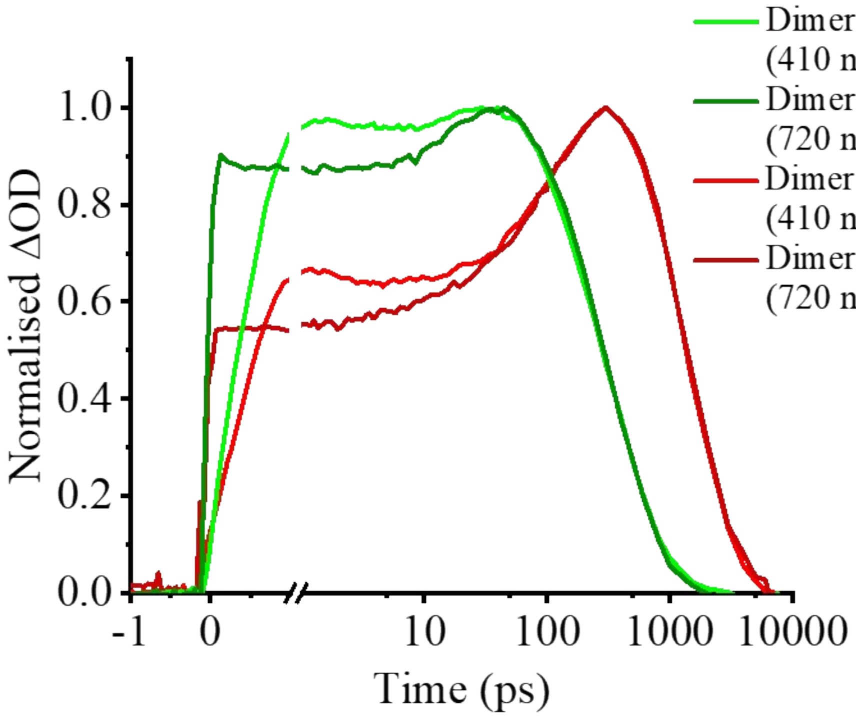

S.I. Fig. 17: Femtosecond transient absorption kinetic trace at 910 nm of dimer I and dimer II in benzonitrile, excited at 410 nm and 720 nm.

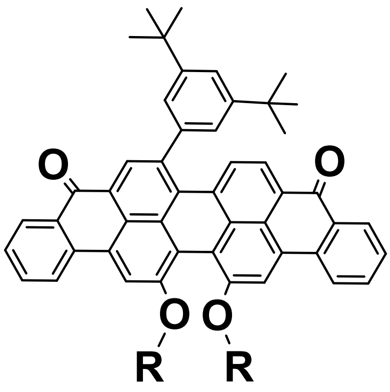

V79-Ar

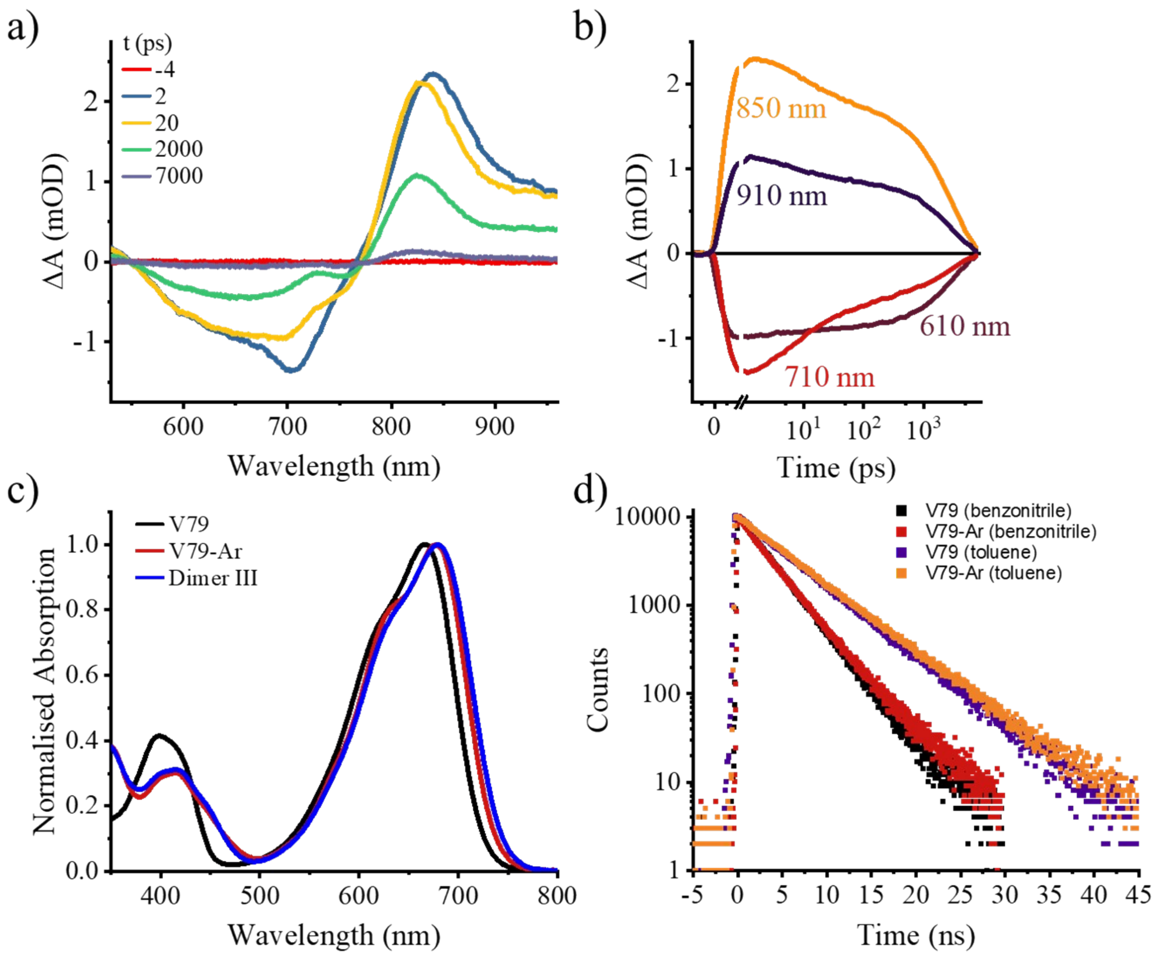

S. I. Fig. 18: Chemical structure and photophysical properties of V79-Ar where: a) femtosecond transient absorption spectra at select time delays of V79-Ar and b) the kinetic traces at select wavelengths in benzonitrile with 410 nm excitation; c) UV/Vis absorption of

V79, V79-Ar and Dimer III in benzonitrile and d) fluorescence decay traces of V79-Ar and V79 in toluene and benzonitrile.

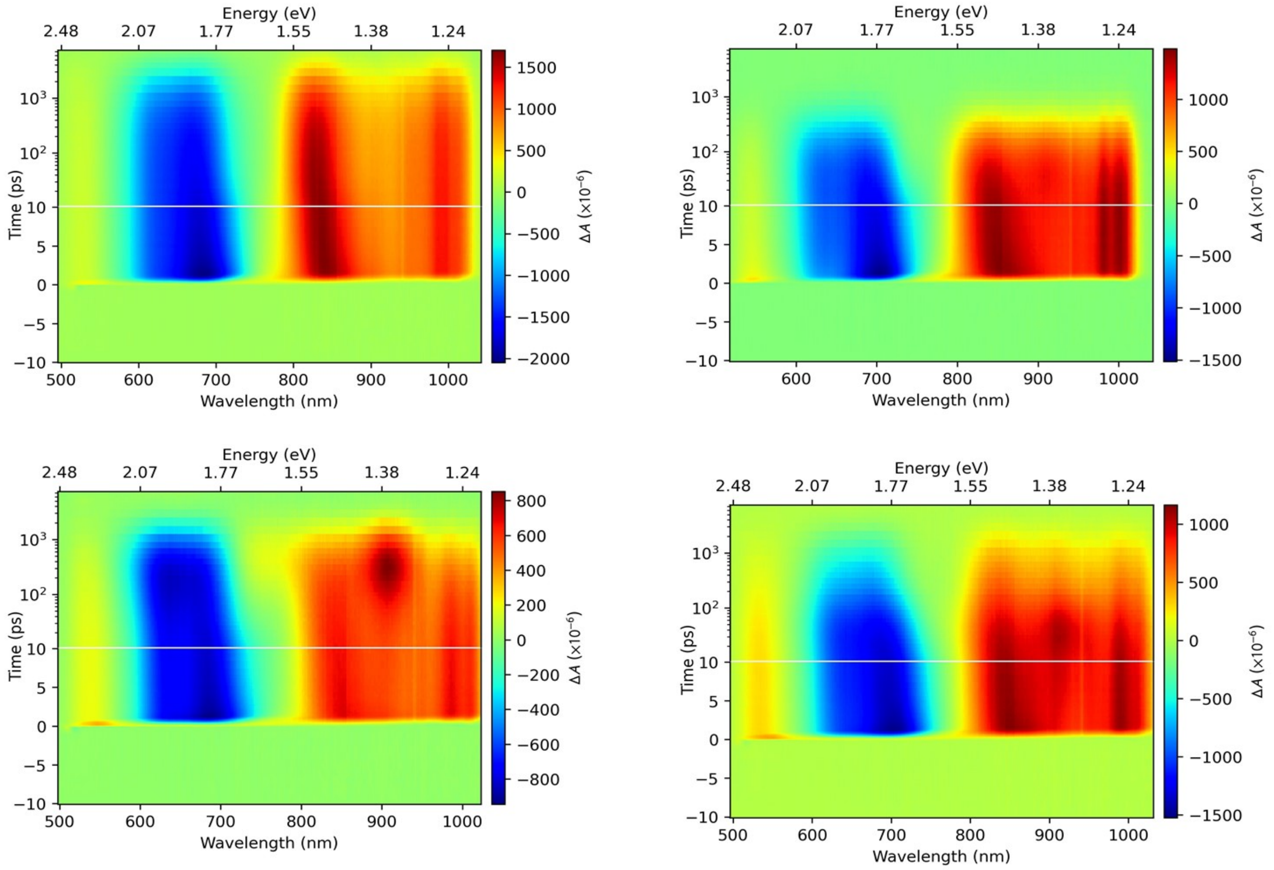

S. I. Fig. 19: 2D plot of femtosecond transient absorption spectra of violanthrone 79 (top left), dimer I (top right), dimer II (bottom left), dimer III (bottom right) in benzonitrile with 410 nm excitation.

S.I. Table 2. Solvent dependent rates of excited state transitions in violanthrone 79 monomer and dimers I, II and III.

		τ_1 (fs)	**k_1 (10^{12} s^{-1})**	**τ_2 (ps)**	**k_2 (10^{10} s^{-1})**	**τ_3 (ps)**	k_3 (10^9 s^{-1})	τ_4 (ns)	k_4 (10^8 s^{-1})
V79	Tol	245	4.1	23	4.4	-	-	5.2	1.9
	BzCN	340	2.9	9	11.1	-	-	3.2	3.1
Dimer I	Tol	260	3.9	40	2.5	-	-	5.4	1.8
	BzCN	610	1.6	26	3.9	350	2.9	-	
Dimer II	Tol	460	2.2	80	1.3	-	-	6.0	1.7
	BzCN	470	2.1	14	7.1	225	4.4	1.2	8.3
Dimer III	Tol	220	4.6	24	4.2	-	-	4.7, 3.3	2.1, 3.0
	BzCN	380	2.6	14	7.1	135	7.4	1.7	5.9

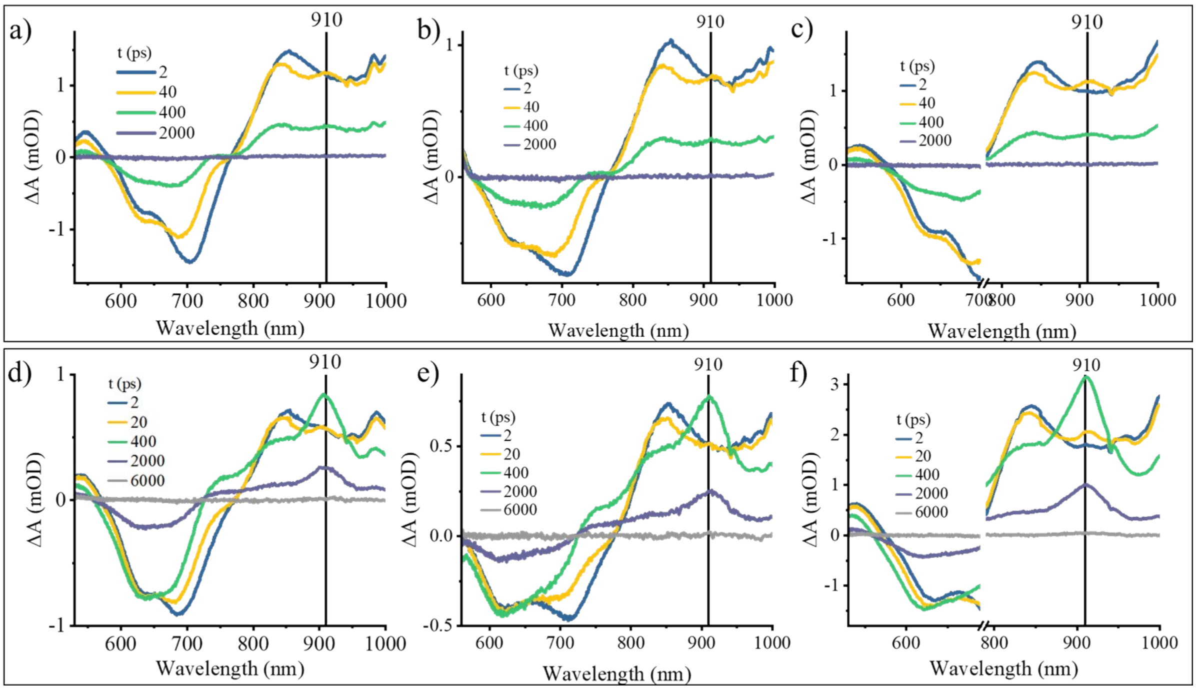

S.I. Fig. 20: Femtosecond transient absorption of dimer Ⅰ (top) and dimer Ⅱ (bottom), in benzonitrile, excited at 410 nm (a and d), 550 nm (b and e) and 720 nm (c and f).

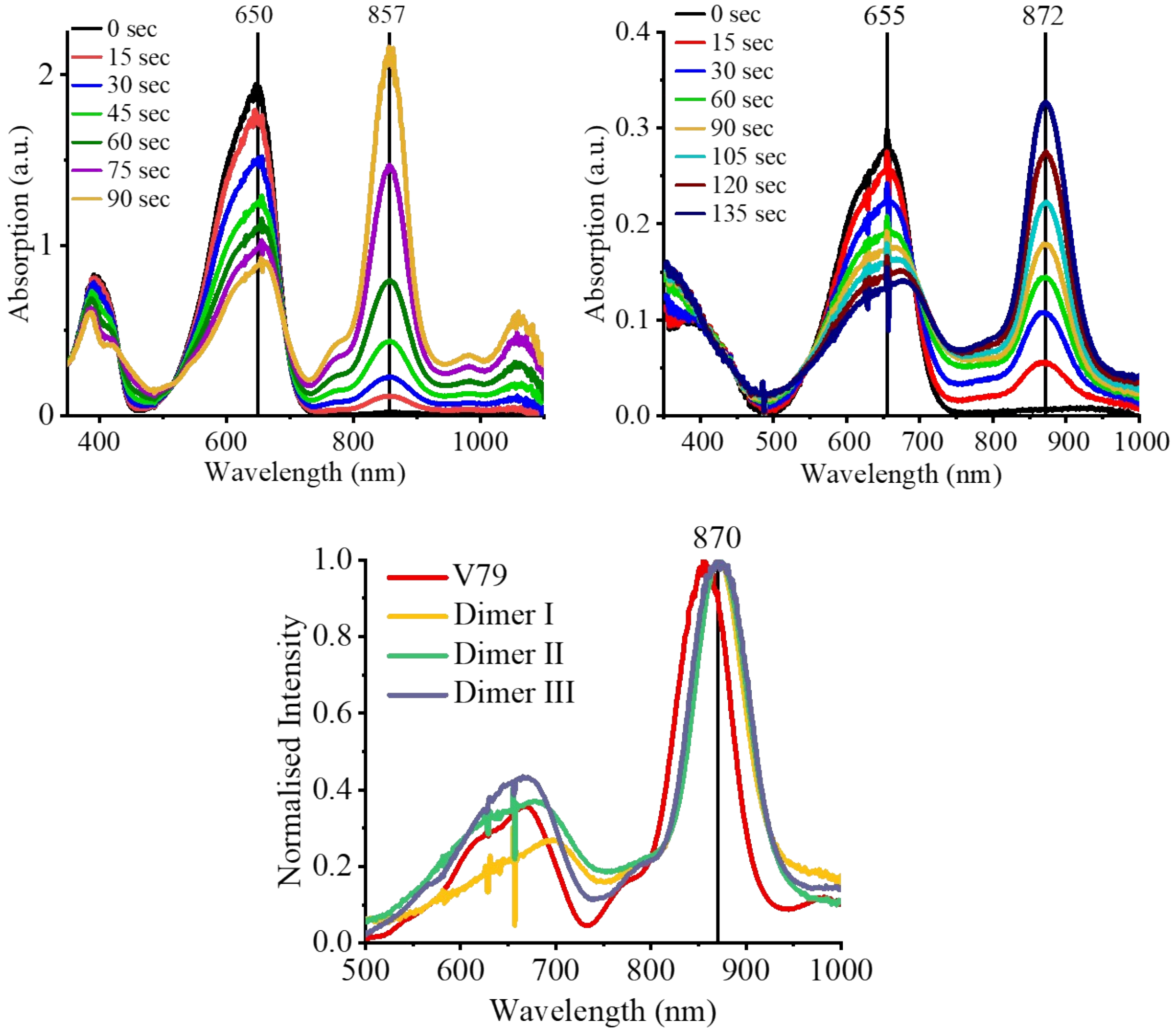

S.I. Fig. 21: UV/Vis obtained during spectroelectrochemical experiments on Violanthrone 79 monomer (top left) and dimer II (top right), in THF with 0.1 M TBAPF$_6$ as electrolyte. Applied voltage was fixed at -1.5 V. The bottom graph shows normalised absorption spectra of all three dimers and a monomer at maximum anion concentration after applied voltage. (Note: The E_{red} of violanthrone is reported as -0.96 eV (NHE) *Ref: Liu, B., Fan, D., Zhang, Q. et al. A novel NIR violanthrone derivative with high electron-deficiency: effect of fluorescence on dicyanomethylene substitution. Front. Chem. China* ***5****, 200–207 (2010).)*

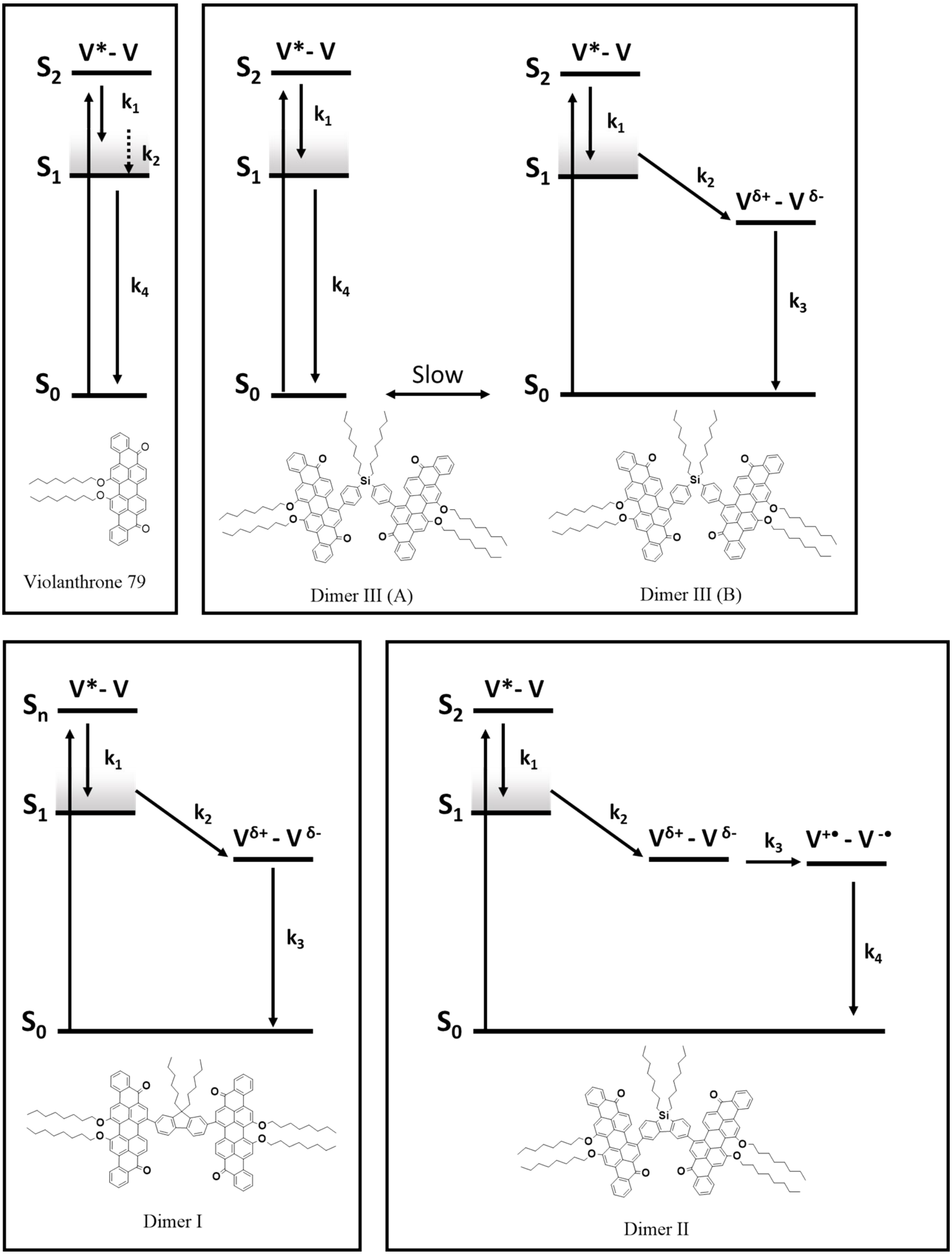

S.I. Fig. 22: Proposed kinetic schemes used to fit TA data of Violanthrone 79 monomer, dimer I, dimer II, and dimer III in polar solvent (benzonitrile).

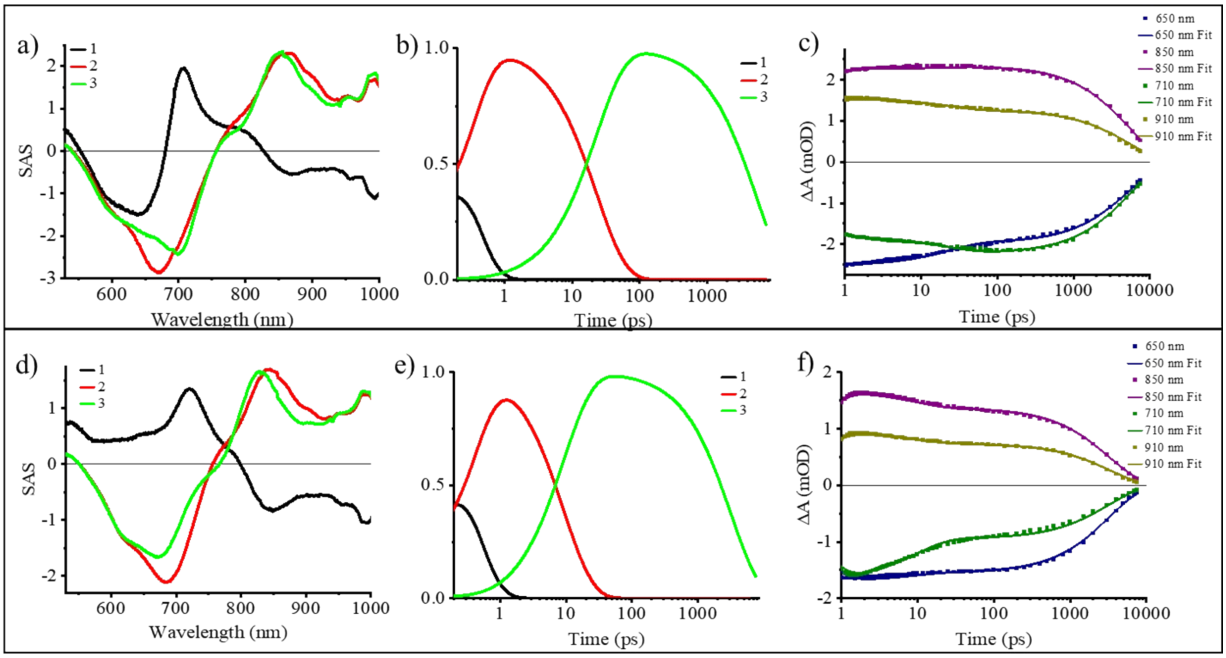

S.I. Fig. 23: Global analysis of femtosecond TA data of violanthrone 79 in toluene (top row) and benzonitrile (bottom row), showing species associated spectra (SAS) of the three components (a and d), temporal evolution of the three components (b and e) and representative kinetic traces at 650 nm, 850 nm, 710 nm and 910 nm and their respective fits (c and f).

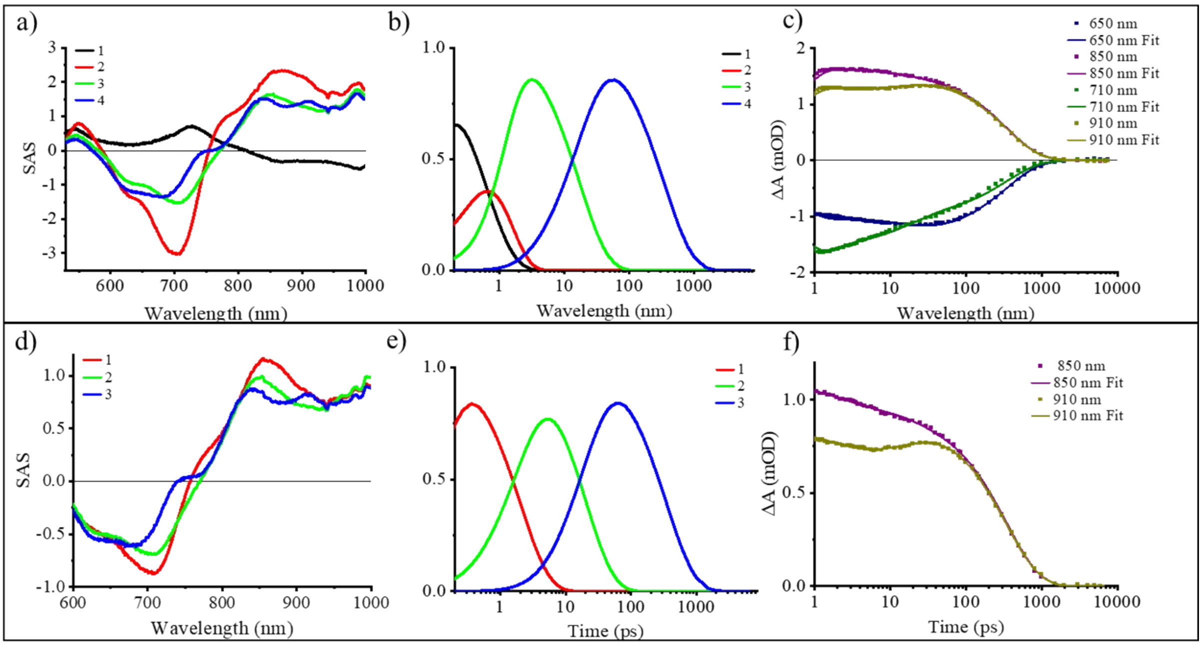

S.I. Fig. 24: Global analysis of femtosecond TA data of Dimer I in benzonitrile with 410 nm excitation (S_n) (top row) and 550 nm excitation (S_1) (bottom row), showing SAS of the components (a and d), temporal evolution of the three components (b and e) and representative kinetic traces at 650 nm, 850 nm, 710 nm and 910 nm and their respective fits (c and f). Deviation in the fit was observed at early time upon excitation into a higher lying excited state and an additional component at early time (not listed in the kinetic scheme) was required to attain reasonable fit. This suggests that additional processes or a different model is required to describe those early interactions. However, a very good fit was obtained for TA data at 550 nm excitation, which captures the dynamics of interest (SBCS) with no CS character observed at those very early times (sub 2 ps). Further work is needed to resolve the interactions occurring upon S_n excitation and will be addressed in future research. Modelled tau and the associated errors from the global analysis of TA data at different pump wavelength are given in the table below:

Dimer I	τ_1 (ps)	τ_2 (ps)	τ_3 (ps)	τ_4 (ps)
410 nm	0.6 (±0.2)	0.6 (±0.2)	17.0 (±0.2)	351 (±0.5)
550 nm		2.0 (±0.2)	20.0 (±0.5)	350 (±0.7)
720 nm			25.6 (±0.7)	353 (±1.2)

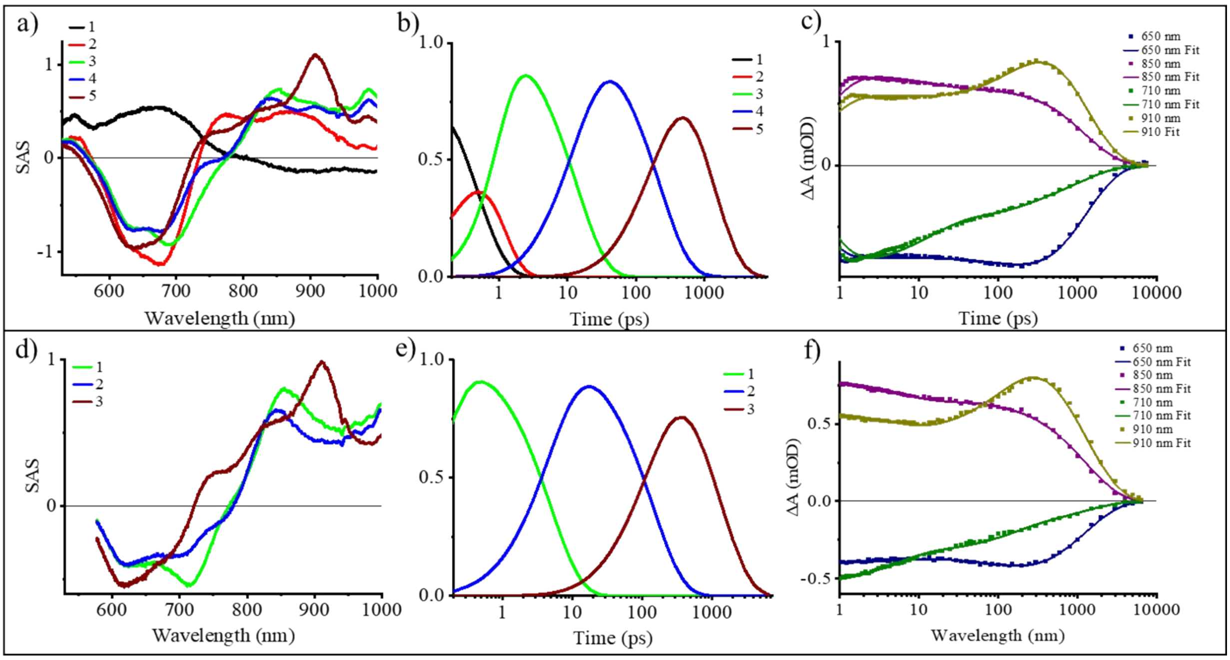

S.I. Fig. 25: Global analysis of femtosecond TA data of Dimer II in benzonitrile with 410 nm excitation (S_2) (top row) and 720 nm excitation (S_1) (bottom row), showing SAS of the components (a and d), temporal evolution of the three components (b and e) and representative kinetic traces at 650 nm, 850 nm, 710 nm and 910 nm and their respective fits (c and f). Slight deviation in the fit was observed at early time upon excitation into a higher lying excited state (S_2) and an additional component at early time (not listed in the kinetic scheme) was required to attain reasonable fit. This suggests that additional processes or a different model is required to describe those early interactions. However, a very good fit was obtained for TA data at 720 nm excitation, which captures the dynamics of interest (SBCT) with no CT character observed at those very early times (sub 2 ps). Further work is needed to resolve the interactions occurring upon S_2 excitation and will be addressed in future research. Modelled tau and the associated errors from the global analysis of TA data at different pump wavelength are given in the table below:

Dimer II	τ_1 (ps)	τ_2 (ps)	τ_3 (ps)	τ_4 (ps)	τ_5 (ns)
410 nm	0.5 (±0.2)	0.5 (±0.2)	13.6 (±0.2)	225 (±2.5)	1.220 (±0.005)
550 nm			5.0 (±0.2)	144 (±1.5)	1.290 (±0.005)
720 nm			1.8 (±0.2)	178 (±1)	1.257 (±0.003)